Catalysis Letters Vol. 99, Nos. 3–4, February 2005 (© 2005)
DOI: 10.1007/s10562-005-2109-5

Thermal and hydrothermal stability of La-modified ETS-10 and its cracking ability

Huifeng Li, Baojian Shen,* Xiaohua Wang and Shikong Shen

State Key Laboratory of Heavy Oil Processing, the Key Laboratory of Catalysis of CNPC, and Faculty of Chemical Engineering, University of Petroleum, Changping, Beijing, and 102249 P.R. China

Received 3 October 2004; accepted 9 November 2004

The ETS-l0 molecular sieve was modified with lanthanum by ion-exchange method. The lanthanum modified ETS-10 shows best thermal and hydrothermal stability in comparison with the as-synthesized ETS-10 and ammonium-exchanged ETS-10. Moreover, the lanthanum modified ETS-10 has an increase in the conversion of *n*-hexadecane by more than 3%, compared with the ammonium-exchanged ETS-10. And the reasonable speculation was presented based on the detailed characterization of these samples by DSC, FT-IR, XRD, XRF and N_2 physisorption.

KEY WORDS: lanthanum; ion-exchange; ETS-10; thermal and hydrothermal stability; cracking ability.

1. Introduction

The unique microporous titanosilicate molecular sieve, ETS-10, consisting of a 3D 12-ring structure, has received considerable attention since it was discovered by Engelhard in 1989 [1]. Moreover, ETS-10 was endowed with special exchange properties and potential catalytic performance for the charge-balancing cations (Na^+ and K^+) on its extra-framework [2–5]. It is well known that, the lanthanum-modified Y zeolite exhibited superior performance in comparison with ammonium exchanged Y zeolite, such as better thermal and hydrothermal stability, stronger acidity [6,7]. To the best of our knowledge, however, the study on the lanthanum-modified ETS-10 was not seen in the open literature.

The aim of our present work is to investigate the effects of lanthanum modification on the thermal and hydrothermal stability and catalytic cracking ability of ETS-10.

2. Experimental

2.1. Catalyst preparation

ETS-10(designated ETS, for convenience) was synthesized using the hydrothermal method [8]. A series of lanthanum-modified ETS-10 (designated HLa1-ETS, HLa2-ETS, HLa3-ETS, respectively) were obtained by means of ion-exchanging of ETS-10 with different amount of lanthanum nitrate in the ammonium nitrate mixed solution, followed by filtering, washing with deionized water, drying at 393 K for 4 h. The corresponding lanthanum contents of HLa1-ETS, HLa2-ETS and HLa3-ETS (calculated by La_2O_3) are 3.04, 3.65 and 4.21 wt% respectively. And the ammonium-exchanged ETS-10 (designated H-Ets) as the reference sample was obtained using the same treatment.

*To whom correspondence should be addressed.
E-mail: baojian@bjpeu.edu.cn

2.2. Characterization

2.2.1. Differential scanning calorimetry

The differential scanning calorimetry (DSC) of the samples were performed on a Netzsch STA 409 simultaneous thermal analysis apparatus. The samples were heated in a Pt-Rh crucible with a heating rate of 10 K/min in argon atmosphere. The flow rate of argon was 20 cm^3/min.

2.2.2. N_2 physisorption

The BET surface area, pore volume, average pore diameter, and pore-size distribution of the samples were determined by N_2 physisorption using a Micromerities ASAP 2020 automated system. Each sample was degassed at 623 K for 5 h prior to N_2 physisorption. The results were given in table 1.

2.2.3. X-ray diffraction

X-ray diffraction patterns were recorded on a SHIMADZU-6000 diffractometer, using the Cu K_α radiation at 40 kV and 30 mA with a scanning rate of 2°/min.

2.2.4. Infrared spectroscopy

Acid sites and acid type distribution were determined by infrared spectroscopy (IR) of chemisorbed pyridine. All spectra were recorded on a MAGNA-IR560ESP Fourier-transform infrared spectrometer at a resolution of 0.35 cm^{-1}. The catalyst samples used for IR were finely ground and pressed into a self-supporting wafer

Table 1
BET surface areas and pore volumes of the samples

Sample	S_{BET} (m^2/g)	V_{total} (cm^3/g)
ETS	391	0.156
H-ETS	378	0.167
HLa1-ETS	352	0.170
HLa1-ETS (after steaming)	260	0.154

(8–10 mg/cm^2, diameter = 15 mm), these were then placed into an infrared cell with KBr windows. The sample degas was carried out at 623 K and 10^{-3}, Pa for 4 h prior to the adsorption of pyridine. IR spectra were recorded after subsequent evacuation at increasing temperatures from 473 to 623 K (1 h at each temperature).

2.2.5. X-ray fluorescence spectroscopy

The lanthanum content was determined on a ZSX100e X-ray fluorescence analyzer.

2.2.6. Thermal stability test

The thermal stability and the crystalline collapse temperatures of ETS, H-ETS and HLa1-ETS, were studied by differential scanning calorimetry (DSC). To further prove, the samples were thermally treated in a furnace in air atmosphere, with the heating rate of 2 K/min, increasing the temperature from room temperature to 923 K and calcining at 923 K for 2 h. Then the retained crystallinity of the corresponding samples was determined by XRD patterns.

2.2.7. Hydrothermal stability test

The hydrothermal stability of ETS, H-ETS and HLa1-ETS, were examined by steam-treated with 100% steam at 873 K for 2 h. Then the retained crystallinity of the corresponding samples was determined by XRD patterns.

2.3. Catalytic tests

The cracking ability of H-ETS, HLa1-ETS, HLa2-ETS and HLa3-ETS (after calcination at 823 K for 4 h in air) with n-hexadecane as the feed, were evaluated on a standard micro-activity test (MAT) unit designed in accordance with ASTM D-3907. Reaction conditions were listed as follows:reaction temperature at 723 K, pressure at atmospheric, weight hourly space velocity of 20 h^{-1} the catalyst loading of 3.0 g, the mass ratio of catalyst to oil of 3. The feed and liquid product were analyzed on a SP 3420 gas chromatograph using a flame ionization detector and a capillary column DM-5(30.0 m × 0.25 mm × 0.32 μm). The conversion of *n*-hexadecane was calculated as follows: Conversion (%) = $[(H_{feed}\text{-}H_{product})/H_{feed}] \times 100$, where H_{feed} and $H_{product}$ indicate the *n*-hexadecane peak area (determined by chromatography analyzes) in the feed and liquid products, respectively.

3. Results and discussion

The DSC curves of ETS, H-ETS and HLa1-ETS were shown in figure 1. Generally, all showed two endothermal peaks, one at low temperature (around 376 K), corresponding to the desorption of water adsorbed in the pores, and another one at high temperature(around 947, 994, and 1013 K, respectively) was corresponding to the phase transition. By contrast, it was evident that the framework of ETS started to collapse at the temperature of 923 K, in agreement with the result reported by Yang and co-workers [8], while the crystalline collapse temperatures of H-ETS and HLa1-ETS, shifted to about 978 and 996 K, respectively. Besides, the XRD patterns of ETS, H-ETS and HLa1-ETS after calcination at 823 K for 5 h were shown in figure 2. All the samples still retained high crystallinity. However, when calcined at 923 K for 2 h; the corresponding XRD patterns (figure 3) recorded, were quite different. The framework of ETS was destroyed completely. And H-ETS also suffered a drastic loss of crystallinity. In contrast, HLa1-ETS still retained a high crystallinity of 49%. Therefore, the thermal stability of the framework is in the order as follows: HLa1-ETS > H-ETS > ETS, confirming the deduction obtained from the DSC curves.

The XRD patterns of ETS, H-ETS and HLa1-ETS after hydrothermal treatment shown in figure 4. It is clear that the crystalline structure of both ETS and H-ETS were seriously degraded, but HLa1-ETS still retained a high crystallinity of 73% and possessed a large surface area of 260 m^2/g, exhibited superior hydrothermal stability. In addition, it is interesting to note that there was a very distinct hysteresis loop on the desorption isotherm of HLa1-ETS after steaming (figure 5), which is characteristic of the existence of mesopores. It means that a secondary pore was generated during the process of hydrothermal treatment. Unexpectedly, however, its total pore volume decreased to some extent, in comparison with that of HLa1-ETS before steaming. This may be ascribed to the crystalline

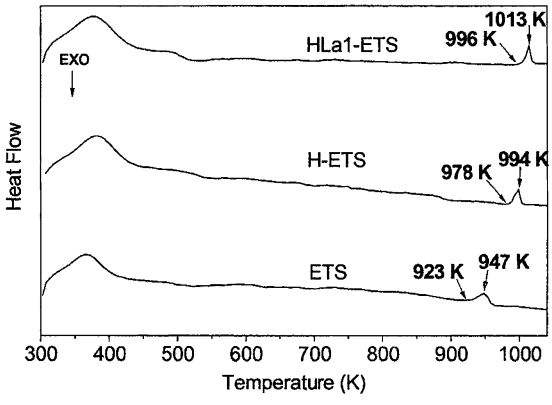

Figure 1. The DSC curves of ETS, H-ETS and HLa1-ETS.

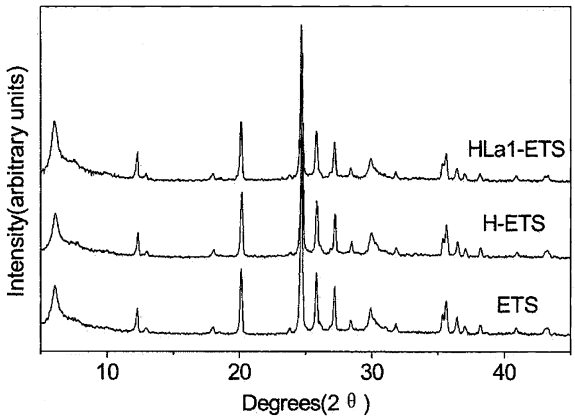

Figure 2. The XRD patterns of ETS, H-ETS and HLa1-ETS after calcinations at 823 K for 5 h in air.

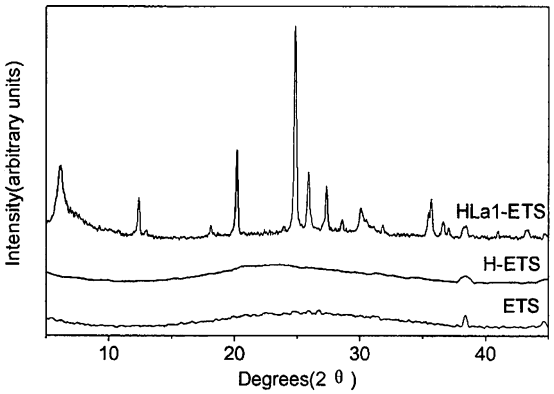

Figure 4. The XRD patterns of ETS, H-ETS and HLa1-ETS after hydrothermal treatment with 100% steam at 873 K for 2 h.

collapse to some extent in the steaming process or the occluded titanium in the channels or pores, due to the partial titanium removal from the framework under severe steaming [9].

According to the accepted explanation for the difference in the stability of NaY, HY, and Rare Earth modified Y [10–12], it can be speculated that the reduced content of sodium and potassium on the extra-framework after ion-exchange, either in ammonium nitrate solution or in the lanthanum nitrate and ammonium nitrate mixed solution, can relieve the deleterious effects of alkaline metals on the stability of framework under severe thermal or hydrothermal treatment. On the other hand, the ammonium-exchange and further calcinations or steam treatments caused the considerable titanium removal from the lattice or the severe distortion of the framework [9], while the additional introduction of lanthanum ion can play an important role in the stabilizing the framework, because after calcination the hydroxyls groups associated with lanthanum ions resulting from the hydrolysis, can preferentially migrate into the main channels of ETS-10 or became parts of its framework, acting as charge compensating cations, which imparted the improved thermal or hydrothermal stability to the framework structure. Besides, the above-mentioned speculation can also be indirectly proved by the comparison of the IR spectra of the hydroxyl groups of H-ETS and HLal-ETS shown in figure 6. It is interesting to find that there is a weak absorption band at 3522.2 cm^{-1} assigned to REOH groups[6,10] appearing in the corresponding IR spectra of HLa1-ETS, and the sharp absorption band at 3737.1 cm^{-1} attributed to silica-like silanol groups is remarkably intensified and noticeably is shifted to 3738.2 cm^{-1}, probably ascribed to the influence of the presence of lanthanum species [6,7,10] in the channels or framework of ETS-10.

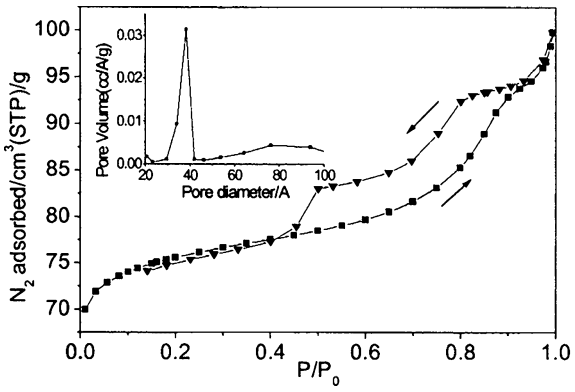

Figure 5. N_2 adsorption and desorption isotherms of HLa1-ETS after steaming. The inlet is its mesopore distribution.

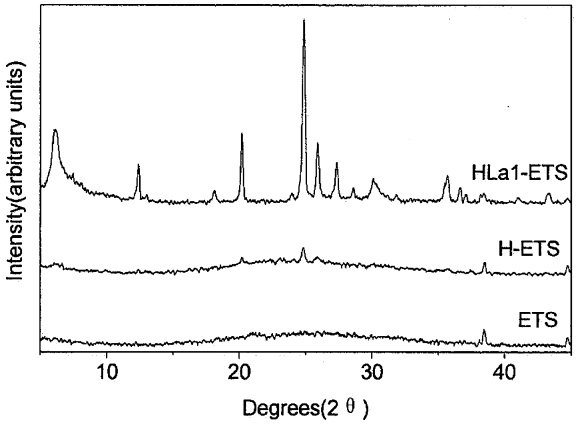

Figure 3. The XRD patterns of ETS, H-ETS and HLa1-ETS after calcinations at 923 K for 2 h in air.

The catalytic cracking activities of H-ETS, HLa1-ETS, HLa2-ETS and HLa3-ETS were presented in figure 7, it is clear that the lanthanum modified ETS-10 possess higher conversion of *n*-hexadecane, with an increase of more than 3% than H-ETS. In addition, it is interesting to find that the catalytic cracking ability of the lanthanum modified ETS-10 is enhanced correspondingly as the increasing lanthanum content. It can

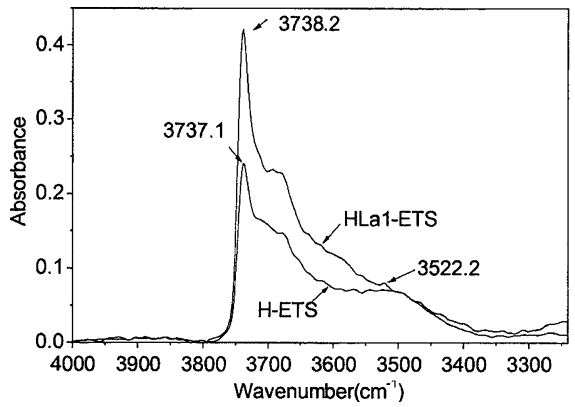

Figure 6. The IR spectra of the hydroxyl groups of H-ETS and HLa1-ETS after evacuation at 623 K and 10^{-3} Pa for 4 h prior to the adsorption of pyridine.

be assumed that the electrostatic fields associated with the multivalent cation (lanthanum ions) were able to polarize adsorbed hydrocarbons sufficiently to promote reaction [7]. Moreover, it was also proved with the results of the acid sites and acid type distribution determined by infrared spectroscopy (IR) of chemisorbed pyridine. The data in table 2 show that the amounts of the B type acid sites and the L type acid sites (pyridine desorption temperature at 473 K) of HLa1-ETS increased correspondingly (It can be speculated that small amounts of adsorbed water in the channels of ETS-10 were partially polarized by the lanthanum ions, with production of acidic hydroxyl groups, either protonic or non-protonic [10]), compared with that of H-ETS. Especially, HLa1-ETS had an notable increase in the amount of the strong-strength L type acid sites (pyridine desorption temperature at 623 K) than H-ETS, while no strong-strength B type acid sites were observed for both (due to the almost complete disappearance of the bridging hydroxyl groups between titanium octahedra and silicon tetrahedra resulting from dehydroxylation processes above 623 K [13]). Based on these results, it was reasonable to arrive at a conclusion

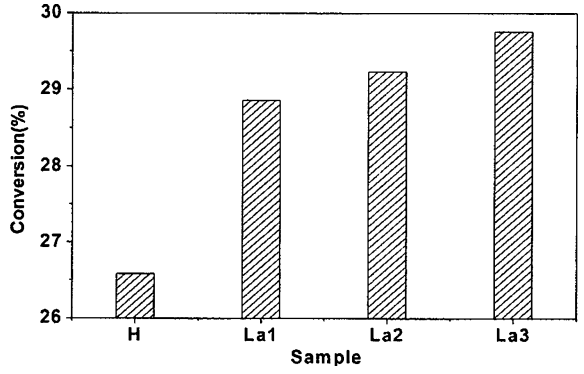

Figure 7. The *n*-hexadecane conversion of the samples: H(H-ETS), La1(HLa1-ETS), La2(HLa2-ETS) and La3(HLa3-ETS).

Table 2
Total acid and acid type distribution of H-ETS and HLa1-ETS

Sample	473 K		623 K	
	B acid (mmol/g)	L acid (mmol/g)	B acid (mmol/g)	L acid (mmol/g)
H-ETS	0.031	0.54	–	0.011
HLa1-ETS	0.040	0.56	–	0.025

that the higher n-hexadecane conversion may be ascribed to the enhanced acid strength and total acid amounts, because the cracking process could also be initiated on a L type acid site via hydride abstraction from a. paraffin, causing the formation of the first surface carbenium ion, then following by the chain propagation, eventually resulting in reaction promotion [7,14–16].

4. Conclusions

The lanthanum modified ETS-10 shows best thermal and hydrothermal stability, in comparison with the as-synthesized ETS-10 and the ammonium-exchanged ETS-10, due to the lanthanum hydroxyl groups migrating into its channels after calcination or acting as the charge balancing cation, which attributing to stabilize the framework of ETS-10. On the other hand, the lanthanum ions can polarize adsorbed hydrocarbons sufficiently to promote reaction, with an increase in the conversion of *n*-hexadecane by more than 3%, compared with the ammonium-exchanged ETS-10.

Acknowledgment

The authors gratefully acknowledge the funding of this project by National Natural Science Foundation of China (Project ID 20276039).

References

[1] S.M. Kuznicki, US patent 4,853,202 (1989).
[2] M.W. Anderson, O. Terasaki, T. Ohsuna, A. Philippou, S.P. Mackay, A. Ferrelra, J. Rocha and S. Lidin, Nature 367 (1994) 347.
[3] D.A. Sommerfeld, W.R. Ellis Jr., E.M. Eyring, S.M. Kuznicki and K.A. Thrush, J. Phys. Chem. 96 (1992) 9975.
[4] S.B. Waghmode, T.K. Das, R. Vetrivel and S. Sivasanker, J. Catal. 185 (1999) 265.
[5] S. Bordiga, C. Pazè, G. Berlier, D. Scarano, G. Spoto, A. Zecchina and C. Lamberti, Catal. Today 70 (2001) 91.
[6] H.G. Karge and H.K. Beyer in:Molecular Sieves, H.G. Karge and Ing. Jens Weitkamp (eds), Vol. 3, (Springer Verlag, Berlin, Heidelberg, 2002) ch. 2.
[7] J.W. Chen and H.C. Cao, *Catalytic Cracking Technology and Engineering* (China petrochemical press, Beijing, 1995).
[8] X. Yang, J.L. Paillaud, H.F.W.J. van Breukelen, H. Kessler and E. Duprey, Micropor. Mesopor. Mat. 46 (2001) 1.

[9] Y. Goa, H. Yoshitake, P. Wu and T. Tatsumi, Micropor. Mesopor. Mat. 70 (2004) 93.
[10] J.W. Ward, J. Phys. Chem. 72 (1968) 4211.
[11] M.L. OcceIli and P. Ritz, Appl. Catal. A 183 (1999) 53.
[12] F.E. Trigueiro, D.F.J. Monteiro, F.M.Z. Zotin and E. Falabella Sousa-Aguiar, J. Alloy. Compd. 344 (2002) 337.
[13] A. Liepold, K. Roos, W. Reschetilowski, Z. Lin, J. Rocha, A. Philippou and M.W. Anderson, Microporous Mater. 10 (1997) 211.
[14] A. Corma, V. Fornés, J.B. Montón and A.V. Orchillés, Ind. Eng. Chem. Prod. Res. Dev. 25 (1986) 231.
[15] A. Corma and A.V. Orchillés, Micropor. Mesopor. Mat. 35 (2000) 21.
[16] A. Brait, A. Koopmans, H. Weinstabl, A. Ecker, K. Seshan and J.A. Lercher, Ind. Eng. Chem. Res. 37 (1998) 873.